Metabolic Engineering 35 (2016) 55–63

Contents lists available at ScienceDirect

Metabolic Engineering

journal homepage: www.elsevier.com/locate/ymben

Original Research Article

Experimental and computational optimization of an *Escherichia coli* co-culture for the efficient production of flavonoids

J. Andrew Jones [a], Victoria R. Vernacchio [a], Andrew L. Sinkoe [c], Shannon M. Collins [a], Mohammad H.A. Ibrahim [d,e], Daniel M. Lachance [b], Juergen Hahn [c], Mattheos A.G. Koffas [a,b,*]

[a] Department of Chemical and Biological Engineering, Rensselaer Polytechnic Institute, Troy, NY 12180, USA
[b] Department of Biological Sciences, Rensselaer Polytechnic Institute, Troy, NY 12180, USA
[c] Department of Biomedical Engineering, Rensselaer Polytechnic Institute, Troy, NY 12180, USA
[d] Department of Chemistry and Chemical Biology, Center for Biotechnology and Interdisciplinary Studies, Rensselaer Polytechnic Institute, Troy, NY 12180, USA
[e] Chemistry of Natural Products Department, National Research Centre, Al-Bohoos St., 12622 Cairo, Egypt

ARTICLE INFO

Article history:
Received 15 November 2015
Received in revised form
13 January 2016
Accepted 14 January 2016
Available online 6 February 2016

Keywords:
Co-culture
Microbial consortium
Flavan-3-ols
Pathway optimization
Systems modeling

ABSTRACT

Metabolic engineering and synthetic biology have enabled the use of microbial production platforms for the renewable production of many high-value natural products. Titers and yields, however, are often too low to result in commercially viable processes. Microbial co-cultures have the ability to distribute metabolic burden and allow for modular specific optimization in a way that is not possible through traditional monoculture fermentation methods. Here, we present an *Escherichia coli* co-culture for the efficient production of flavonoids *in vivo*, resulting in a 970-fold improvement in titer of flavan-3-ols over previously published monoculture production. To accomplish this improvement in titer, factors such as strain compatibility, carbon source, temperature, induction point, and inoculation ratio were initially optimized. The development of an empirical scaled-Gaussian model based on the initial optimization data was then implemented to predict the optimum point for the system. Experimental verification of the model predictions resulted in a 65% improvement in titer, to 40.7 ± 0.1 mg/L flavan-3-ols, over the previous optimum. Overall, this study demonstrates the first application of the co-culture production of flavonoids, the most in-depth co-culture optimization to date, and the first application of empirical systems modeling for improvement of titers from a co-culture system.

1. Introduction

The microbial production of biofuels, commodity chemicals, and natural products is continually being improved through the use of various pathway optimization tools and techniques (Boock et al., 2015; Cress et al., 2015b; Jones et al., 2015b). Until recently, these efforts have focused primarily on optimization of single strain monocultures to facilitate conversion of substrate to product. Although successful, these efforts are continually plagued with the trade-offs associated with choosing a single host strain to simultaneously perform multiple bioconversions, often having different precursor and co-factor requirements (Yadav et al., 2012). Nature has overcome these trade-offs through organelle compartmentalization of pathways in higher organisms (Roze et al., 2011) and through microbial consortia in lower organisms (Koenig et al., 2011; Paerl and Pinckney, 1996). Humans have taken advantage of co-culture approaches for wastewater treatment (Gaikwad et al., 2014; Manz et al., 1994) and fermented food products (Smid and Lacroix, 2013; Young and Kiefer, 2014) for decades. However, only recently have scientists begun to investigate the true potential of co-culture techniques in metabolic engineering and synthetic biology applications (Brenner et al., 2008).

Recently, several groups have reported elegant applications utilizing co-cultures for the production of pharmaceutical precursors (Zhou et al., 2015), commodity chemicals (Zhang et al., 2015a, 2015b), and potential biofuels (Saini et al., 2015). In one such

* Corresponding author at: Rensselaer Polytechnic Institute, 110 8th Street, Troy, NY 12180, USA.
E-mail addresses: jonesj12@rpi.edu (J.A. Jones), vernav@rpi.edu (V.R. Vernacchio), sinkoa@rpi.edu (A.L. Sinkoe), collis6@rpi.edu (S.M. Collins), ibrahm3@rpi.edu (M.H.A. Ibrahim), lachad2@rpi.edu (D.M. Lachance), hahnj@rpi.edu (J. Hahn), koffam@rpi.edu (M.A.G. Koffas).

http://dx.doi.org/10.1016/j.ymben.2016.01.006
1096-7176/

example, a *Saccharomyces cerevisiae–Escherichia coli* co-culture was engineered to take advantage of rapid taxadiene production from *E. coli* and the ability of *S. cerevisiae* to actively express cytochrome P450s to catalyze taxadiene functionalization into oxygenated taxanes. These steps have proven to be inefficient or impossible to accomplish in either a *S. cerevisiae* or *E. coli* monoculture. Albeit impressive, previous studies have lacked the rigorous optimization necessary to fully realize the complete production potential of these co-culture systems.

We report the development and optimization of an *E. coli–E. coli* co-culture for the efficient production of flavonoids. Flavonoids are high-value molecules with promising potential for pharmaceutical applications resulting from interesting bioactivity (Chemler et al., 2007; Bhan et al 2013; Heiss et al., 2003; Hooper et al., 2012; Monagas et al., 2010). In the case of flavan-3-ols, a subclass of flavonoid molecules, high-titer production has been achieved from both the malonyl-CoA requiring upstream module (phenylpropanoic acids to flavanones) (Leonard et al., 2007; Xu et al., 2011) and the NADPH requiring downstream module (flavanones to flavan-3-ols) (Zhao et al., 2015). However, when the complete pathway is expressed in monoculture, reported titers for flavan-3-ols from phenylpropanoic acids are greater than three orders of magnitude lower than the independent modules (Chemler et al., 2007). This observation motivated the choice to attempt co-culture production of flavan-3-ols in *E. coli*.

To accomplish this task, careful experimental optimization of carbon source, induction temperature, induction point, inoculation ratio, and strain choice was used to map the production landscape. The experimental optimization was coupled with extensive empirical modeling techniques that were applied to predict conditions for optimal production. Searching the solution space surrounding the predicted optimum resulted in a 65% improvement in flavan-3-ol titer to 40.7 ± 0.1 mg/L from *p*-coumaric acid, representing a 970-fold improvement over previous literature reports. This study highlights the potential for the use of co-culture methods to further improve microbial production of plant natural products in *E. coli*.

2. Materials and methods

2.1. Bacterial Strains, vectors, and media

E. coli DH5α was used to propagate all plasmids, while the BL21star™(DE3), BL21star™(DE3)Δ*suc*CΔ*fumC*, or BL21star™(DE3) Δ*pgi*Δ*ppc* was used as the hosts for flavonoid production (Chemler et al., 2010). The ePathBrick vector, pETM6, was used as the basis for all plasmid construction and pathway expression. Luria Broth (LB) Lennox modification (Sigma) and Andrew's Magic Medium (AMM) (He et al., 2015) were used where noted. All plasmid constructs will be made available through Addgene.org.

2.2. Flavonoid pathways and ePathOptimize library construction

Genes involved in the 12 candidate upstream flavanone production pathways were obtained from previously published literature from the Koffas lab. *Vv*4CL, *Pc*4CL, *Cm*CHS, *Ph*CHS, *Cm*CHI, and *Ms*CHI were obtained in ePathBrick vector pETM6 (Cress et al., 2015a; Xu et al., 2012), while *At*4CL was acquired through PCR amplification (ACCUZYME 2x mix, Bioline) of plasmid #3 DNA using primers 1 and 2 (Supplementary Table 2) (Lim et al., 2011). The ePathBrick destination vector, pETM6, and *At*4CL PCR amplicon were digested with restriction enzymes *Nde*I/*Xho*I (FastDigest, Thermo Scientific) and gel purified (E.Z.N.A. MicroElute Gel Extraction Kit, Omega Bio-tek). Digested *At*4CL PCR product was ligated with digested pETM6 backbone to create plasmid 2, Supplementary Table 1. Constructs were then transformed into chemically competent DH5α for verification and plasmid propagation. Colonies were screened via restriction digest and further verified with Sanger sequencing (GENEWIZ, Inc.) using the sequencing primers 3 and 4 in Supplementary Table 2. Site directed mutagenesis was then preformed using standard protocols to silently remove the *Nhe*I restriction site from *At*4CL using primers 5 and 6 (Supplementary Table 2). Complete candidate pathways were constructed in monocistronic form using standard ePathBrick methods (Xu et al., 2012) resulting in plasmids 10–27, Supplementary Table 1. Occasionally the restriction site *Apa*I was used to replace *Sal*I when the pathway genes either contained internal *Sal*I restriction sites or to optimize the insert:backbone ratio for improved ligation efficiency. Plasmids p148 and p168 containing complete downstream modules were not modified from previous reports (Zhao et al., 2015).

The upstream pathway genes were cloned in monocistronic form with randomized promoter strengths using previously published methods (Jones et al., 2015). Multiple transformations were oftentimes completed to ensure sufficient library sampling and retention. The final plasmid library, pETM6-xx*At*4CL-xx*Ph*CHS-xx*Cm*CHI, was transformed into BL21star™(DE3)Δ*sucC*Δ*fumC* for screening. The 'xx' feature represents the inclusion of a single random mutant T7 promoter from the five-member ePathOptimize library.

2.3. Small-scale cultivation protocol

Single colonies of each strain were inoculated separately into 25 mL of AMM in a 125 mL non-baffled shake flask with ampicillin (80 μg/mL) and grown overnight at 37 °C. After 14 h, the overnight cultures were mixed volumetrically to the indicated inoculation ratios and were inoculated at 2% (40 uL) into 2 mL of AMM and allowed to grow at 37 °C before induction with 1 mM IPTG. Upon induction, the cultures were transferred to the appropriate induction temperature and grown for 48 h. All small-scale screening was completed in polypropylene 48-well plates (5 mL, VWR). Except where noted, the cultures were grown in AMM with 20 g/L Glycerol, 100 mg/L of substrate was added at induction, and 30 °C was used as the induction temperature.

2.4. Bioreactor fermentation protocol

Fed-batch style fermentation was performed using a DASGIP parallel bioreactor at an initial working volume of 500 mL of AMM with 20 g/L glycerol as a carbon source. Overnight cultures were prepared identically to the small-scale protocol presented above. The bioreactor was inoculated at an initial ratio of 7:3 (C5:p168) at 2% of final volume. The pH and DO of the fermentation broth was maintained at 7.2 and 50 percent saturation through addition of 6 M sodium hydroxide and application of stirring cascade control, respectively. The feed solution [250 g/L glycerol, 4 g/L casamino acids, 7 g/L $(NH_4)_2HPO_4$, and 80 μg/mL ampicillin] and 2x MOPS mix (Jones et al., 2015) was fed at 2 mL per hour from 5–15 h and 4 mL per hour from 15–26 h. The fermentation was induced with IPTG to a final concentration of 1 mM after 7 h of growth ($OD_{600}=7.1$) and the system was cooled to 30 °C. The substrate, p-coumaric acid, was added in 50 mg/L aliquots at 1, 4, and 7 h post induction. Samples were taken periodically for measurement of OD_{600} and metabolite analysis.

2.5. Metabolite analysis

Fermentation broth was mixed with an equal volume of absolute ethanol and vortexed for 10 seconds prior to centrifugation (10 min, 20,000*g*). The supernatant (25 μL) was used for HPLC

analysis carried out using Agilent 1200 series HPLC equipped with a ZORBAX SB-18 column (5 μm, 4.6 × 150 mm) and a diode array detector. The mobile phase was acetonitrile (solvent A) and water (solvent B) (both contain 0.1% formic acid) at a flow rate of 1 mL/min. HPLC program was as follows: 10–40% A (0–10 min) and 40–60% A (10–15 min). Absorbance at 280 nm was monitored in all cases. Titer of products was determined using authentic standards while (+)-afzelechin was quantified using the (+)-catechin calibration curve. All experiments were preformed in duplicate. Error bars represent ±1 standard deviation of biological duplicate. Significance of data was determined using a two-tailed unpaired *t*-test with a 95% confidence interval.

2.6. Empirical modeling methods

The empirical model function used is a four-dimensional scaled-Gaussian function of the form

$$y(x) = \frac{b}{\sqrt{(2\pi)^4|\Sigma|}} e^{-\frac{1}{2}(x-\mu)^T\Sigma^{-1}(x-\mu)}$$

where the parameters are $\Sigma \in \mathbb{R}^{4\times4}$, $\mu \in \mathbb{R}^{4\times1}$, and $b \in \mathbb{R}$; and $x \in \mathbb{R}^{4\times1}$ contains the values of the experimental variables: induction point, inoculation ratio, carbon source, induction temperature. Parameter values were determined by least squares using 72 experimental data points. Fitted parameter values are listed in Supplementary Table 3. The empirical model was optimized to find the maximum titer $y(x)$ by varying x. The optimization was performed by equivalently minimizing $-y(x)$ using the MATLAB function fmincon, which utilizes an interior point method to find the minimum of a constrained nonlinear multivariable function. All calculations involved in parameter fitting and optimization of the empirical function were carried out in MATLAB, and scripts can be viewed in Supplementary materials.

3. Results and discussion

The production of flavan-3-ols from phenylpropanoic acid precursors proceeds through six enzymatic steps: 4-coumaroyl-CoA ligase, 4CL; chalcone synthase, CHS; chalcone isomerase, CHI; flavanone 3β-hydroxylase, F3H; dihydroflavonol 4-reductase, DFR; leucoanthocyanidin reductase, LAR; (Fig. 1). The complete pathway is partitioned such that both the upstream and downstream modules contain three genes. This modularization reduces the metabolic burden of enzyme overexpression and divides the pathway according to necessary co-factor requirements: malonyl-CoA (upstream) and NADPH (downstream).

3.1. Independent optimization of upstream and downstream modules

The ability to tailor the genetic optimization of each strain in a co-culture system for improved flux towards necessary co-factors and substrates through the pathway of interest and away from unwanted side products is a major advantage over monoculture methods. We began our modular optimization by focusing on the upstream strain containing 4CL, CHS, and CHI. Building on previous efforts to optimize malonyl-CoA availability, BL21star™(DE3) Δ*sucC*Δ*fumC* was chosen as the host strain for this upstream module (Xu et al., 2011). We then chose homologs for each of the three enzymes from different plant sources, resulting in 12 combinations of potential upstream pathways. Upon screening for functional conversion of two phenylpropanoic acid precursors to

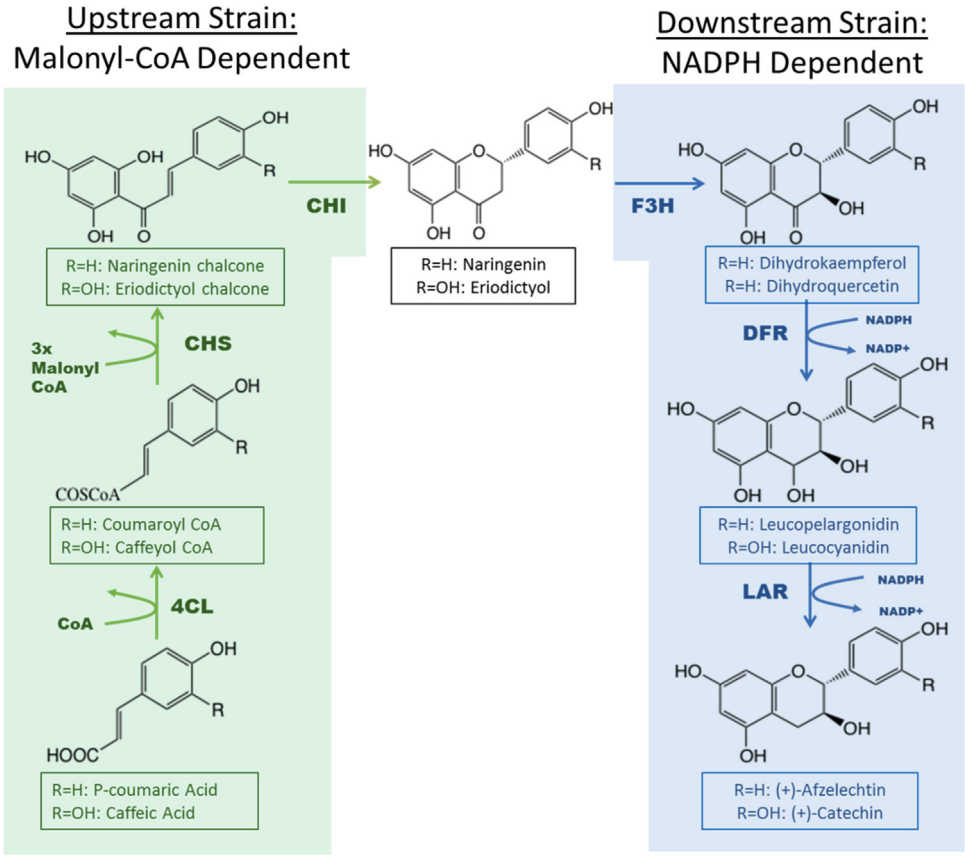

Fig. 1. Flavonoid pathway highlighting upstream (green) malonyl-CoA dependent and downstream (blue) NADPH dependent co-culture modules. (For interpretation of the references to color in this figure legend, the reader is referred to the web version of this article.)

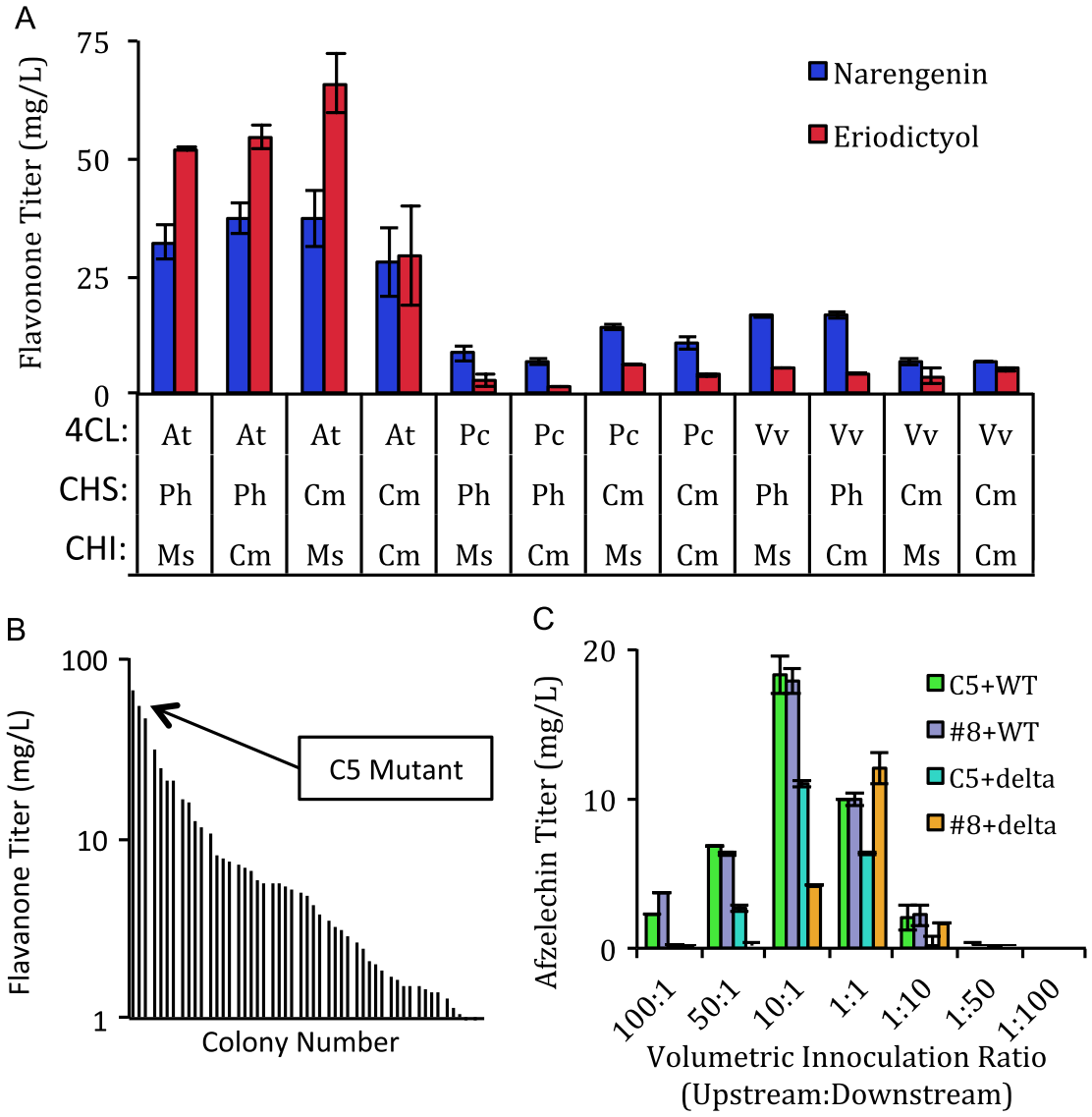

Fig. 2. Upstream strain optimization and co-culture compatibility determination. (A) Screening of 12 potential upstream homolog combinations resulted in several high-titer pathways. (B) Application of ePathOptimize technique for transcriptional optimization resulted in high sensitivity to changes in the transcriptional landscape. (C) Lead strains from the individual strain optimization studies were grown in co-culture to determine strain compatibility prior to additional fermentation optimization. All data was obtained in AMM – 2% glucose, 30 °C induction temperature. Error bar represent ± one standard deviation from duplicate experiments.

their corresponding flavanones, several high-titer homolog combinations were discovered (Fig. 2A). Constructs containing the 4CL from *Arabidopsis thaliana* (*At*4CL) showed significantly ($p < 0.001$) higher conversion leading towards the choice of construct containing *At*4CL, *Ph*CHS, and *Cm*CHI for further optimization.

Using the recently published ePathOptimize technique for modulating the transcriptional landscape (Jones et al., 2015), the promoter strengths of each gene in the upstream module were randomized to one of five mutant T7 promoters of various strength. The library members were then screened for conversion of *p*-coumaric acid to naringenin *in vivo* (Fig. 2B). The results indicated high sensitivity to promoter strength and resulted in one mutant (C5 or pFlavo^{opt}) that out-performed the consensus T7 control strain by 24%. This pFlavo^{opt} mutant was sequenced and was found to have the consensus T7 sequence controlling expression of *At*4CL and *Ph*CHS, while the strong mutant promoter C4 was found to control expression of *Cm*CHI. The nomenclature C5 or pFlavo^{opt} refers to the transcriptionally optimized plasmid expressed in the flavanone expression strain BL21starTM(DE3) (S4, Supplementary Table 1) and contains the incorporation of ePathOptimize mutant T7 promoter C4 controlling the expression of CmCHI. This transcriptionally optimized plasmid was then utilized in future co-cultures.

Optimization of the downstream pathway has been previously explored through screening of 18 homolog gene combinations resulting in two combinations that exhibit efficient conversion of both naringenin and eriodictyol substrates across a wide range of substrate concentrations (Zhao et al., 2015). To confirm the findings of this previous study, both the p148 and p168 constructs were tested using a cultivation protocol and substrate concentration realistic to the levels expected in the current study. Similar titers and trends were obtained with p168 slightly out-performing p148 (Supplementary Fig. 1), leading towards the choice of p168 for the downstream module in the co-culture optimization. Further optimization of plasmid p168 was not performed due to limiting fluxes through the upstream module. With independent genetic optimization of the upstream and downstream modules completed, the lead candidates for each module were then screened for strain compatibility in co-culture.

3.2. Determination of co-culture compatibility

Strain compatibility is a significant factor in any co-culture system. The strains must be able to efficiently grow in the same media, have the same antibiotic selection, and must not produce toxic compounds that significantly harm the other members of the microbial community. Many of these criteria can be easily addressed by using strains of similar background, but module specific mutations towards improving intercellular conditions for the pathway of interest can impact cellular compatibility in co-culture. Furthermore, pathway metabolites that connect the individual members of the co-culture must be readily transferred across the cell membrane from the producer to the consumer.

Two strains from each the upstream and downstream module were tested for their cross compatibility in co-culture. For the upstream strain, the transcriptionally optimized pFlavo^{opt} mutant and the consensus control plasmid (#17, Supplementary Table 1) were used in strain BL21star™(DE3)Δ*sucC*Δ*fumC*, while for the downstream module a single plasmid, p168, was tested in two host strains: wild type BL21star™(DE3) and BL21star™(DE3) Δ*pgi*Δ*ppc*. The authors have noticed a significant decrease in cell growth for the Δ*pgi*Δ*ppc* strain background and hypothesized that this would affect strain performance in co-culture. Four co-culture combinations were tested across various initial inoculation cell ratios (Fig. 2C) and a significant reduction in flavan-3-ol titer was seen for the two co-cultures containing BL21*(DE3)Δ*pgi*Δ*ppc* ($p < 0.001$). Nearly identical performance was achieved by strains containing either the consensus control or the pFlavo^{opt} mutant upstream module. From these results, the authors chose BL21*(DE3)Δ*sucC*Δ*fumC* with the pFlavo^{opt} mutant upstream module and the wild type BL21*(DE3) with the p168 plasmid for further optimization.

3.3. Determination of important optimization parameters

To begin fermentation optimization of the co-culture system, we identified two key parameters predicted to result in high sensitivity: induction point and inoculation ratio. Both the upstream and downstream modules contain pET expression cassettes controlled by the T7-*lac* system, and therefore protein production is inducible with the addition of IPTG. A wide variety of optimum induction points have been presented in the primary literature for pET-based systems indicating that the optimum induction point is linked to division of cellular resources and is more complex than purely affecting protein production levels (Andrianantoandro et al., 2006; Jones et al., 2015a). Due to this complexity, the optimum induction point is specific to the particular system and set of cultivation conditions and must be determined experimentally.

The initial inoculation ratio of upstream to downstream cells in the fermentation is another important parameter that adds to the complexity of co-culture systems. Variation of this ratio allows for changes to be made in population dynamics, accounting for differences in population growth rate and specific activity of the strains in co-culture. Interestingly, when various induction points were crossed with multiple inoculation ratios, we saw an orthogonal response in product titer from the two parameters (Fig. 3A). The system demonstrated a peak induction point of 4 h post-inoculation regardless of inoculation ratio and a peak inoculation ratio of 9:1 regardless of induction point, resulting in the point of highest titer at a 4-h induction and an initial inoculation ratio of

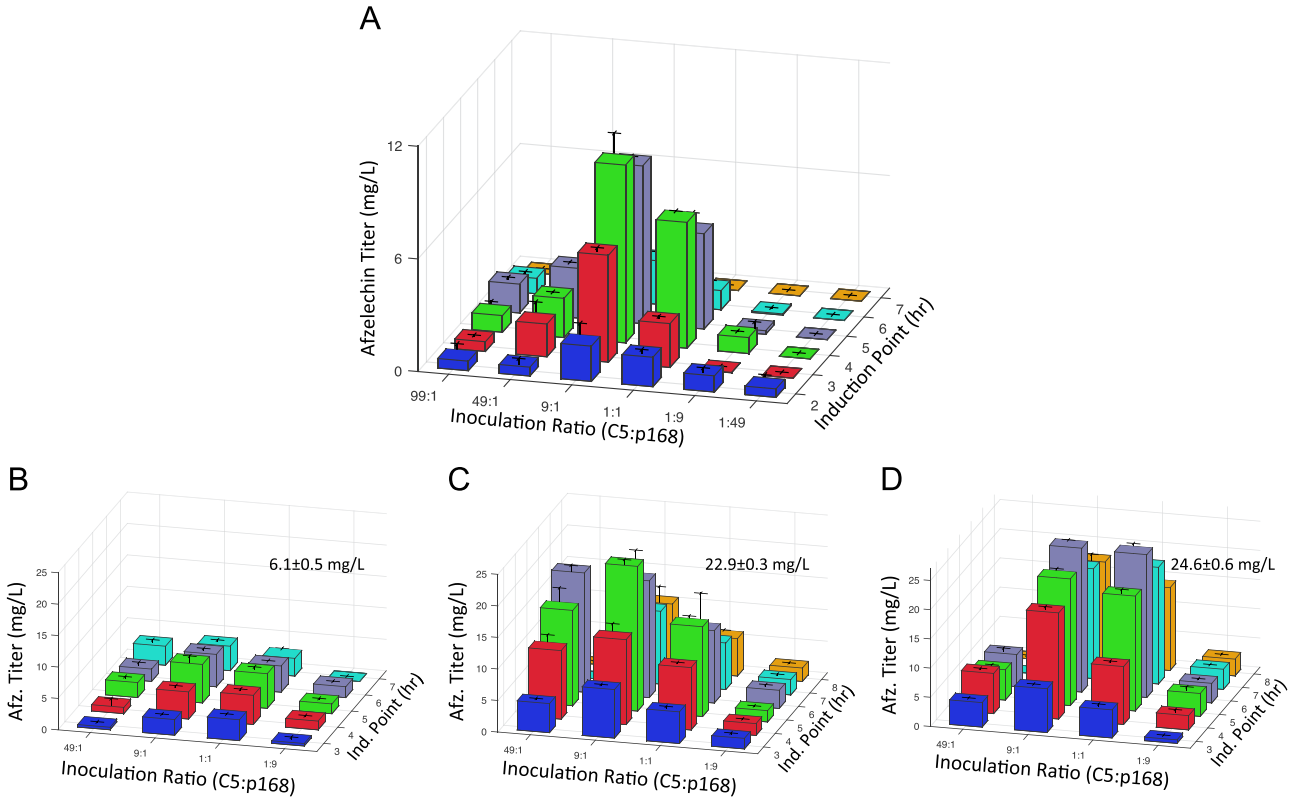

Fig. 3. Sensitivity to induction point, inoculation ratio, and induction temperature for the co-culture system. (A) Variations in induction point and inoculation ratio demonstrate orthogonal response in product titer. Data obtained in glucose only media at an induction temperature of 30 °C. (B–D) Variations in the induction temperature show significant shifts to the magnitude and profile of the production landscape. Data obtained in glycerol only media. (B) 10 °C induction temperature. (C) 20 °C induction temperature. (D) 30 °C induction temperature. Data labels represent the highest titer reported in each window. Error bars represent ± one standard deviation from duplicate or greater ($n \geq 2$) experiments.

9:1 (C5:p168). This finding led to the decision to screen all future parameters across various induction points and inoculation ratios to visualize the production landscape. Furthermore, the observed trends indicate that the system is stable over a wide range of initial inoculation ratios, showing no tipping point where one strain demonstrates a propensity to dominate the population with time. Additional analysis of substrate and flavanone intermediate concentrations also vary as expected with variable inoculation ratio (Supplementary Fig. 2). In co-cultures with dominant upstream ratios, considerable initial substrate is utilized and intermediate product is accumulated, but little intermediate is converted to final product; while co-cultures with dominant downstream ratios utilized little initial substrate, limiting flux through the entire system. However, at intermediate inoculation ratios, high amounts of initial substrate are utilized while low intermediate product titers are present due to efficient conversion to the final product.

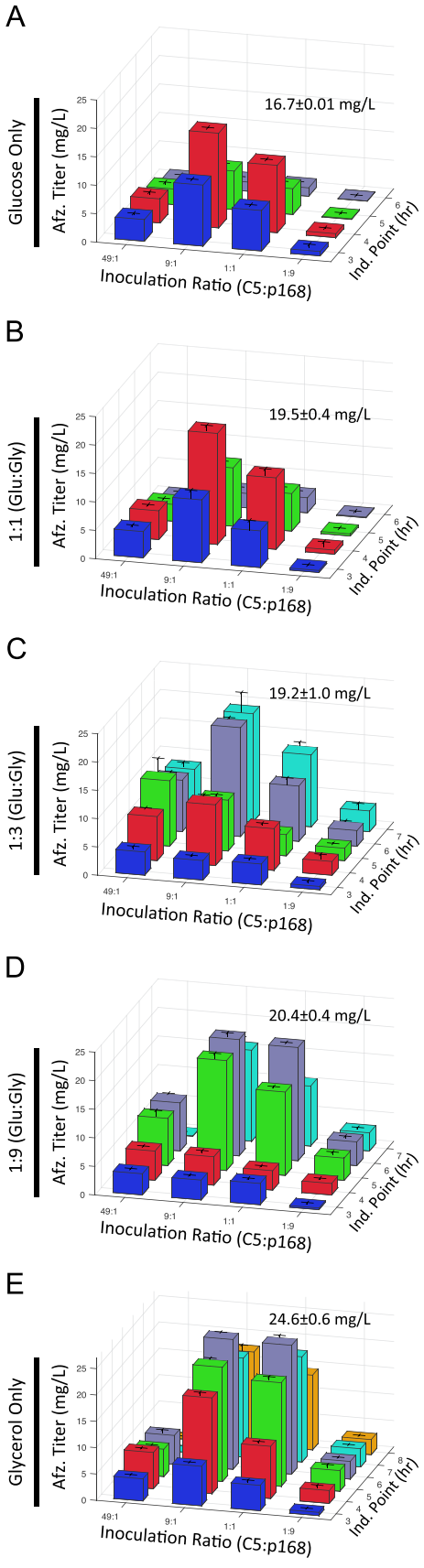

Fig. 4. Effect of carbon source composition on product titer and the shape of the production landscape. (A–E) Increasing the proportion of glycerol in the production media results in higher titers, later induction point optimums, and optimum inoculation ratios with higher proportion of the downstream strain. (A) Glucose Only. (B) 1:1 Glucose:Glycerol. (C) 1:3 Glucose:Glycerol. (D) 1:9 Glucose:Glycerol. (E) Glycerol Only. Data labels represent the highest titer reported in each window. Error bars represent ± one standard deviation from duplicate or greater ($n \geq 2$) experiments.

3.4. *Effect of carbon source*

Previous literature reports and early experimental evidence (data not shown) fueled the decision to use the Andrew's Magic Medium (AMM) with 20 g/L of glucose as the initial production media for individual strain optimization and preliminary co-culture experiments. In an attempt to reduce the production costs at the industrial scale, and because of the increased interest to utilize glycerol for industrial fermentations (Da Silva et al., 2009; Martínez-Gómez et al., 2012), we varied the proportion of glucose to glycerol in the culture media. In addition to economic incentives, the preference for glycerol over other carbon sources has been reported for different microbial strains due to strain-specific differences in gene expression and metabolite profiles upon growth on glycerol (Bizzini et al., 2010). With all media having 20 g/L total carbon source, five carbon source ratios were tested ranging from glucose only to glycerol only (Fig. 4A–E). Several trends in the production landscape were observed upon the shift from growth on glucose to glycerol. The most noticeable trend was higher optimum titers with increasing proportion of glycerol. Upon growth on increasing proportions of glycerol, a shift in the production landscape resulted in higher titers appearing at later induction points and peak inoculation ratios with higher proportion of the downstream strain. Additionally, glucose-grown cultures demonstrate a sharp peak in the production landscape, where glycerol-grown cultures show a plateau with many high-titer solutions.

3.5. *Induction temperature optimization*

Fermentation temperature can affect cellular growth dynamics, enzyme folding, and specific enzyme activity (Hannig and Makrides, 1998). These effects have not been well documented on the systems level, such that optimum fermentation temperature could be predicted for any given system *a priori*. We therefore decided to test co-culture production at induction temperatures of 10, 20, or 30 °C. The co-culture was grown at 37 °C prior to induction at which the temperature was then dropped to the specified induction temperature after induction. Previous efforts have maintained an induction temperature of 30 °C. A significant decrease in optimal titer was observed in the 10 °C case with the 20 and 30 °C cases showing similar maximum achieved titers (Fig. 3B–D). Although similar in optimum titer, the 20 and 30 °C cases did show different production landscapes such that the 20 °C

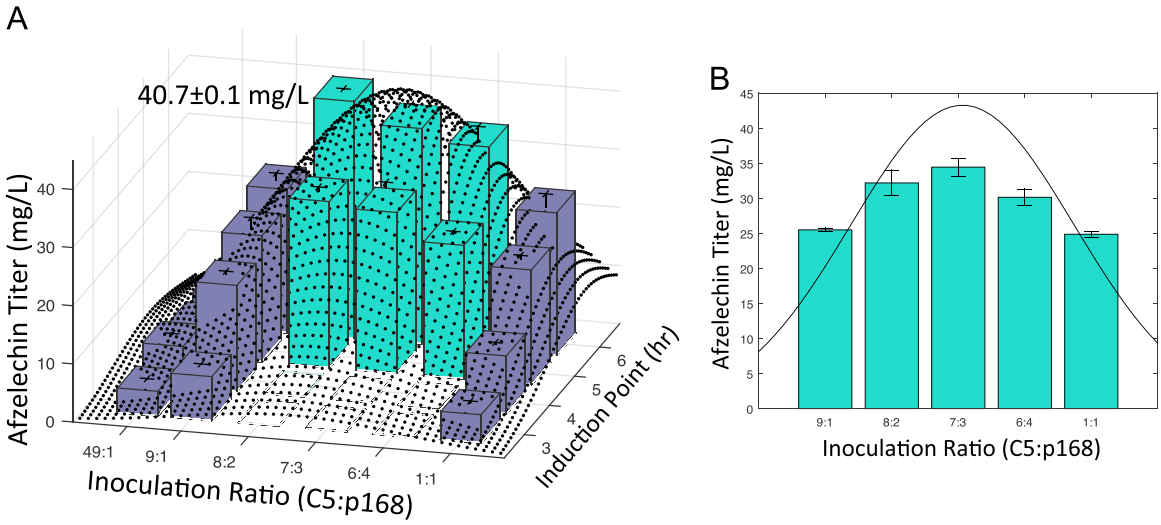

Fig. 5. Experimental points vs. model predictions for the co-culture system. Columns represent experimental data points, while the surface plot (black) represents the model-predicted production landscape. Purple columns represent data included in the model training set, while green columns represent the points selected for model validation. Data were measured at an induction temperature of 30 °C in 20 g/L glycerol media. (A) 3D comparison of model predicted vs. experimentally determined production landscape. (B) Comparison of experimental data to model at model predicted optimum induction point, 5.67 h. Error bars represent ± one standard deviation from duplicate or greater ($n \geq 2$) experiments. (For interpretation of the references to color in this figure legend, the reader is referred to the web version of this article.)

case had a sharp optimum while the 30 °C case demonstrated more of a plateau with many conditions resulting in moderately high titers. Additionally, similar trends were observed for increasing induction temperature as were seen for increasing proportion of glycerol in the media. Notably, increases in induction temperature resulted in a shift of the production landscape towards optimum solutions with later induction points and inoculation ratios favoring more of the downstream strain.

3.6. System modeling for prediction of optimum operating conditions

The aforementioned observations suggested that the titer achieved by the system could be improved by selecting optimized experimental conditions. To identify potential conditions that could result in an optimal titer, an empirical modeling approach was utilized (Bhadouria et al., 2014; Dai et al., 2014). Due to the trends observed from preliminary data showing the dependence of titer on induction point, inoculation ratio, carbon source, and induction temperature, we constructed an empirical scaled-Gaussian model, which uses these four experimental variables as inputs and computes the titer. This model contains 21 parameters that were fitted using 72 experimental data points. In particular, titer was measured at each combination of the following: induction point – 3, 4, 5, 6 h; inoculation ratio (upstream:downstream) – 49:1, 9:1, 1:1; carbon source (glucose:glycerol) – 1:0, 1:1, 0:1; induction temperature – 20, 30 °C. The model demonstrates a close fit with the training data, and follows the general trend of additional data that were not used for model fitting (Fig. 5). The optimal point of the model function was determined computationally, and was used to direct future experiments in search of optimal operating conditions to maximize titer. Interestingly, the optimal point of the model function was found to be at operating conditions not tested previously, and within a gap between previously tested experimental points. Specifically, the optimal conditions predicted by the model were: induction point of 5.5 h; inoculation ratio of 7:3 (upstream:downstream); carbon source ratio of 0:1 (glucose:glycerol); and induction temperature of 25 °C.

Experiments were subsequently performed at conditions in the region of the model-predicted optimum (Fig. 5 and Supplementary Fig. 3). These experiments resulted in a maximum titer of 40.7 ± 0.1 mg/L, a 65% increase over the highest titer measured prior to computational optimization. This maximal titer was achieved experimentally at an induction point of 6 h; inoculation ratio of 8:2 (upstream:downstream); carbon source ratio of 0:1 (glucose:glycerol); and induction temperature of 30 °C. This point was within the set of experimental points we tested based on proximity with the model-predicted optimum, but the point differs slightly from the model-predicted optimum. This is not surprising, as a scaled-Gaussian model was used for fitting the data and computing the optimum, whereas the behavior of the true system is likely more complex than can be fully captured by such an empirical model. That being said, using a scaled-Gaussian model represented a good trade-off between model complexity and quality of fit for the available data, and the model was ultimately successful in guiding experiments to achieve substantially higher titers. This suggests that relatively simple empirical models can be effective tools for informing titer optimization efforts.

3.7. Bioreactor scale-up: proof of principle

To demonstrate the stability and scalability of our co-culture system, we show scale-up of the fermentation from a 2 mL culture in a 48-well plate directly to a bioreactor with a 500 mL working volume. Utilizing near optimum conditions from previous small-scale optimization experiments, the bioreactor demonstrated slightly lower (34 vs. 41 mg/L) product titers than that of the optimized small-scale system (Supplementary Fig. 4). We predict this is due to a shift in the production landscape as a result of scale-up but believe that global trends due to induction point, inoculation ratio, media composition, and induction temperature will remain constant for the system. The additional control gained through the use of bioreactors also results in additional complexity from a pathway optimization standpoint. To that end, the complete fermentation optimization of our co-culture system is beyond the scope of this work but represents a promising direction for future optimization studies.

4. Conclusions

The ability to harness the power of multiple strains in co-culture allows for a division of metabolic burden across the

population, as well as the ability to genetically optimize each module individually for specific co-factor and precursor requirements. Through exploitation of these advantages and empirical modeling techniques, we were able to improve production of flavonoids to 40.7 ± 0.1 mg/L, a 970-fold improvement over previous monoculture efforts. These results suggest that future attempts to expand to poly-culture production, with three or more strains in co-culture, should be addressed from a tandem systems modeling/experimental approach.

Conflicts of interest

The authors declare no conflicts of interest.

Author contributions

JAJ, VRV, ALS, and MHAI designed research; JAJ, VRV, SMC, ALS, MAHI, and DML performed research; JAJ and ALS analyzed data; JAJ, ALS, JH, and MAGK wrote the paper; JH and MAGK supervised the research.

Acknowledgments

The authors would like to acknowledge funding from the RPI Biocatalysis and Metabolic Engineering Constellation Fund.

Appendix A. Supplementary material

Supplementary data associated with this article can be found in the online version at http://dx.doi.org/10.1016/j.ymben.2016.01.006.

References

Andrianantoandro, E., Basu, S., Karig, D.K., Weiss, R., 2006. Synthetic biology: new engineering rules for an emerging discipline. Mol. Syst. Biol. 2. http://dx.doi.org/10.1038/msb4100073.

Bhadouria, A.S., Sorci, M., Gu, M., Belfort, G., Hahn, J., 2014. Optimization of membrane separation processes for protein fractionation. Ind. Eng. Chem. Res. 53, 5103–5109. http://dx.doi.org/10.1021/ie401303d.

Bhan, N., Xu, P., Koffas, M.A., 2013. Pathway and protein engineering approaches to produce novel and commodity small molecules. Curr. Opin. Biotechnol. 26, 1137–1143. http://dx.doi.org/10.1016/j.cobio.2013.02.019.

Bizzini, A., Zhao, C., Budin-Verneuil, A., Sauvageot, N., Giard, J.-C., Auffray, Y., Hartke, A., 2010. Glycerol is metabolized in a complex and strain-dependent manner in *Enterococcus faecalis*. J. Bacteriol. 192, 779–785. http://dx.doi.org/10.1128/JB.00959–09.

Boock, J.T., Gupta, A., Prather, K.L., 2015. Screening and modular design for metabolic pathway optimization. Curr. Opin. Biotechnol. 36, 189–198. http://dx.doi.org/10.1016/j.copbio.2015.08.013.

Brenner, K., You, L., Arnold, F.H., 2008. Engineering microbial consortia: a new frontier in synthetic biology. Trends Biotechnol. 26, 483–489. http://dx.doi.org/10.1016/j.tibtech.2008.05.004.

Chemler, J.A., Lock, L.T., Koffas, M.A.G., Tzanakakis, E.S., 2007. Standardized biosynthesis of flavan-3-ols with effects on pancreatic beta-cell insulin secretion. Appl. Microbiol. Biotechnol. 77, 797–807. http://dx.doi.org/10.1007/s00253–007–1227-y.

Chemler, J.A., Fowler, Z.L., McHugh, K.P., Koffas, M.A., 2010. Improving NADPH availability for natural product biosynthesis in *Escherichia coli* by metabolic engineering. Metab. Eng. 12, 96–104. http://dx.doi.org/10.1016/j.ymben.2009.07.003.

Cress, B.F., Trantas, E.A., Ververidis, F., Linhardt, R.J., Koffas, M.A., 2015b. Sensitive cells: enabling tools for static and dynamic control of microbial metabolic pathways. Curr. Opin. Biotechnol. 36, 205–214. http://dx.doi.org/10.1016/j.copbio.2015.09.007.

Cress, B.F., Toparlak, Ö.D., Guleria, S., Lebovich, M., Stieglitz, J.T., Englaender, J.A., Jones, M.A.G., Linhardt, R.J., Koffas, M.A.G., 2015a. CRISPathBrick: modular combinatorial assembly of Type II-A CRISPR arrays for dCas9-mediated multiplex transcriptional repression in *E. coli*. ACS Synth. Biol. 4, 987–1000. http://dx.doi.org/10.1021/acssynbio.5b00012.

Dai, W., Word, D.P., Hahn, J., 2014. Modeling and dynamic optimization of fuel-grade ethanol fermentation using fed-batch process. Control Eng. Pract. 22, 231–241. http://dx.doi.org/10.1016/j.conengprac.2013.01.005.

Gaikwad, G.L., Wate, S.R., Ramteke, D.S., Roychoudhury, K., 2014. Development of microbial consortia for the effective treatment of complex wastewater. J. Bioremediat. Biodegrad., 05. http://dx.doi.org/10.4172/2155–6199.1000227.

Hannig, G., Makrides, S.C., 1998. Strategies for optimizing heterologous protein expression in *Escherichia coli*. Trends Biotechnol. 16, 54–60. http://dx.doi.org/10.1016/S0167–7799(97)01155-4.

He, W., Fu, L., Li, G., Andrew Jones, J., Linhardt, R.J., Koffas, M., 2015. Production of chondroitin in metabolically engineered *E. coli*. Metab. Eng. 27, 92–100. http://dx.doi.org/10.1016/j.ymben.2014.11.003.

Heiss, C., Dejam, A., Kleinbongard, P., Schewe, T., Sies, H., Kelm, M., 2003. Vascular effects of cocoa rich in flavan-3-ols. JAMA 290, 1030–1031. http://dx.doi.org/10.1001/jama.290.8.1030.

Hooper, L., Kay, C., Abdelhamid, A., Kroon, P.A., Cohn, J.S., Rimm, E.B., Cassidy, A., 2012. Effects of chocolate, cocoa, and flavan-3-ols on cardiovascular health: a systematic review and meta-analysis of randomized trials. Am. J. Clin. Nutr. 95, 740–751. http://dx.doi.org/10.3945/ajcn.111.023457.

Jones, J.A., Toparlak, Ö.D., Koffas, M.A., 2015b. Metabolic pathway balancing and its role in the production of biofuels and chemicals. Curr. Opin. Biotechnol. 33, 52–59. http://dx.doi.org/10.1016/j.copbio.2014.11.013.

Jones, J.A., Collins, S.M., Lachance, D.M., Vernacchio, V.R., Koffas, M.A.G., 2015a. Optimization of naringenin and p -coumaric acid hydroxylation using the native *E. coli* hydroxylase complex, HpaBC. Biotechnol. Prog. n/a–n/a . http://dx.doi.org/10.1002/btpr.2185.

Jones, J.A., Vernacchio, V.R., Lachance, D.M., Lebovich, M., Fu, L., Shirke, A.N., Schultz, V.L., Cress, B., Linhardt, R.J., Koffas, M.A.G., 2015. ePathOptimize: a combinatorial approach for transcriptional balancing of metabolic pathways. Sci. Rep. 5, 11301. http://dx.doi.org/10.1038/srep11301.

Koenig, J.E., Spor, A., Scalfone, N., Fricker, A.D., Stombaugh, J., Knight, R., Angenent, L.T., Ley, R.E., 2011. Succession of microbial consortia in the developing infant gut microbiome. Proc. Natl. Acad. Sci. USA 108, 4578–4585. http://dx.doi.org/10.1073/pnas.1000081107.

Leonard, E., Lim, K.H., Saw, P.N., Koffas, M.A., 2007. Engineering central metabolic pathways for high-level flavonoid production in *Escherichia coli*. Appl. Environ. Microbiol. 73, 3877–3886.

Lim, C.G., Fowler, Z.L., Hueller, T., Schaffer, S., Koffas, M.A.G., 2011. High-yield resveratrol production in engineered *Escherichia coli*. Appl. Environ. Microbiol. 77, 3451–3460. http://dx.doi.org/10.1128/AEM.02186–10.

Manz, W., Wagner, M., Amann, R., Schleifer, K.-H., 1994. In situ characterization of the microbial consortia active in two wastewater treatment plants. Water Res. 28, 1715–1723. http://dx.doi.org/10.1016/0043–1354(94)90243-7.

Martínez-Gómez, K., Flores, N., Castañeda, H.M., Martínez-Batallar, G., Hernández-Chávez, G., Ramírez, O.T., Gosset, G., Encarnación, S., Bolivar, F., 2012. New insights into *Escherichia coli* metabolism: carbon scavenging, acetate metabolism and carbon recycling responses during growth on glycerol. Microb. Cell Fact. 11, 46. http://dx.doi.org/10.1186/1475–2859–11–46.

Monagas, M., Urpi-Sarda, M., Sánchez-Patán, F., Llorach, R., Garrido, I., Gómez-Cordovés, C., Andres-Lacueva, C., Bartolomé, B., 2010. Insights into the metabolism and microbial biotransformation of dietary flavan-3-ols and the bioactivity of their metabolites. Food Funct. 1, 233. http://dx.doi.org/10.1039/c0fo00132e.

Paerl, H.W., Pinckney, J.L., 1996. A mini-review of microbial consortia: their roles in aquatic production and biogeochemical cycling. Microb. Ecol. 31. http://dx.doi.org/10.1007/BF00171569.

Roze, L.V., Chanda, A., Linz, J.E., 2011. Compartmentalization and molecular traffic in secondary metabolism: a new understanding of established cellular processes. Fungal Genet. Biol. 48, 35–48. http://dx.doi.org/10.1016/j.fgb.2010.05.006.

Saini, M., Hong Chen, M., Chiang, C.-J., Chao, Y.-P., 2015. Potential production platform of n-butanol in *Escherichia coli*. Metab. Eng. 27, 76–82. http://dx.doi.org/10.1016/j.ymben.2014.11.001.

da Silva, G.P., Mack, M., Contiero, J., 2009. Glycerol: a promising and abundant carbon source for industrial microbiology. Biotechnol. Adv. 27, 30–39. http://dx.doi.org/10.1016/j.biotechadv.2008.07.006.

Smid, E.J., Lacroix, C., 2013. Microbe-microbe interactions in mixed culture food fermentations. Curr. Opin. Biotechnol. 24, 148–154. http://dx.doi.org/10.1016/j.copbio.2012.11.007.

Xu, P., Vansiri, A., Bhan, N., Koffas, M.A.G., 2012. ePathBrick: a synthetic biology platform for engineering metabolic pathways in *E. coli*. ACS Synth. Biol. 1, 256–266. http://dx.doi.org/10.1021/sb300016b.

Xu, P., Ranganathan, S., Fowler, Z.L., Maranas, C.D., Koffas, M. a G., 2011. Genome-scale metabolic network modeling results in minimal interventions that cooperatively force carbon flux towards malonyl-CoA. Metab. Eng. 13, 578–587. http://dx.doi.org/10.1016/j.ymben.2011.06.008.

Yadav, V.G., De Mey, M., Giaw Lim, C., Kumaran Ajikumar, P., Stephanopoulos, G., 2012. The future of metabolic engineering and synthetic biology: towards a systematic practice. Metab. Eng. 14, 233–241. http://dx.doi.org/10.1016/j.ymben.2012.02.001.

Young, V.A., Kiefer, A.M., 2014. Kimchi: spicy science for the undergraduate microbiology laboratory. J. Microbiol. Biol. Educ 15, 297–298. http://dx.doi.org/10.1128/jmbe.v15i2.695.

Zhang, H., Li, Z., Pereira, B., Stephanopoulos, G., 2015a. Engineering *E. coli–E. coli* cocultures for production of muconic acid from glycerol. Microb. Cell Fact. 14, 134. http://dx.doi.org/10.1186/s12934−015−0319-0.

Zhang, H., Pereira, B., Li, Z., Stephanopoulos, G., 2015b. Engineering *Escherichia coli* coculture systems for the production of biochemical products. Proc. Natl. Acad. Sci. USA 112, 8266–8271. http://dx.doi.org/10.1073/pnas.1506781112.

Zhao, S., Jones, J.A., Lachance, D.M., Bhan, N., Khalidi, O., Venkataraman, S., Wang, Z., Koffas, M.A.G., 2015. Improvement of catechin production in *Escherichia coli* through combinatorial metabolic engineering. Metab. Eng. 28, 43–53. http://dx.doi.org/10.1016/j.ymben.2014.12.002.

Zhou, K., Qiao, K., Edgar, S., Stephanopoulos, G., 2015. Distributing a metabolic pathway among a microbial consortium enhances production of natural products. Nat. Biotechnol. 33, 377–383. http://dx.doi.org/10.1038/nbt.3095.